Modified embedded-atom method used to derive interatomic potentials for defects and phase formation in the W-C system

P. H. Chen[1,2,*] and K. Nordlund[1]

[1]*Accelerator Laboratory, University of Helsinki, P.O. Box 43, 00014 Helsinki, Finland*

[2]*Science and Technology on Surface Physics and Chemistry Laboratory, P.O. Box 718-35, 621907 Mianyang, China*

(Received 16 July 2013; published 2 December 2013)

An interatomic potential for the W-C system has been derived based on the second-nearest-neighbor modified embedded-atom method scheme. The potential parameters were constructed by fitting to the experimental information on the formation energy of interstitial carbon atoms, the migration energy of carbon atoms in body-centered-cubic (bcc) tungsten and lattice parameters, bulk modulus, and cohesive energy of B_h W_2C carbide. We demonstrate that such potential can not only reproduce the behavior of carbon atoms in bcc tungsten, but also be employed for modeling energetics and structural properties of tungsten carbides. Moreover, this potential is used to study the stability of multicarbon-multivacancy (C_nV_m) clusters in bcc tungsten. The binding energy and configurations of C_nV_m clusters that were not attainable with existing potentials or identified previously via *ab initio* methods are proposed. Results show that carbon atoms can be strongly trapped by vacancies and interstitials in bcc W. Such bonding between carbon and vacancies lead to the formation of C_nV_m complexes and influence the physical properties of metallic tungsten. Besides, a positive binding energy of C-C cluster and C-SIA clusters was found, and both clusters form a hexagonal WC-like local structure. This result provides a plausible explanation for the experimentally observed formation of hexagonal WC (not W_2C) in bcc W.

DOI: 10.1103/PhysRevB.88.214101 PACS number(s): 61.50.Lt, 61.72.jn, 62.20.D−, 31.15.xv

I. INTRODUCTION

Tungsten (W) and its alloys are the most promising plasma-facing material (PFM) in the future fusion reactor, at least in the divertor region, due to their low sputtering erosion and good thermal properties.[1,2] For the International Thermonuclear Experimental Reactor (ITER), tungsten will be used at baffles and side-wall regions of the divertor plates, together with carbon (C) at the strike points of the divertor plates.[3] C impurities have been found to interact strongly with various defects such as vacancies, self-interstitials, dislocations, and grain boundaries in numerous metals and alloys. The mixing of W and C, even a very small amount of C impurity atoms, can change the thermal and mechanical characteristics significantly.[4]

Multicarbon-multivacancy clusters (C_nV_m) play an important role in the degradation of thermal and mechanical property of tungsten.[4] However, the atomistic properties of C_nV_m in metals are difficult to identify experimentally due to their small size. Although these point defect clusters are critical to the properties of tungsten, the material physics that governs interactions between interstitial atoms and vacancies remains poorly understood. Atomistic simulation provides a useful tool to study the evolution of defects in metals. Several works[5–7] have been reported on the interaction of C with vacancies in W by first-principles methods, and reveal some detailed information on the defect structures in bcc W. However, due to the size limit, only information on small C_nV_m ($n < 5, m < 2$) clusters are provided. It is usually too slow to deal with large clusters ($n > 10, m > 3$) by first-principles calculations. Another approach is to use empirical interatomic potentials to perform molecular dynamics (MD) simulation, which can provide valuable insight for macroscale materials models. Bond order potentials (BOPs) for W-C systems have been developed by Juslin *et al.*[8] This potential reproduces most crystalline properties very well, but provides a poor description on the interaction between carbon atoms and defects in tungsten matrix. For example, the migration energy of C atoms in bcc W was found to be about 0.34 eV, whereas the lowest experimental value is about 1.64 eV.[9] A successful MD simulation usually depends on reliable interatomic potential, which should not only be able to reproduce crystalline properties, but also provide accurate descriptions of the interaction between interstitials and crystalline defects. For this purpose, a second-nearest-neighbor modified embedded-atom method potential (2NN MEAM) for the W-C system which can describe the physical properties of alloys over the entire composition range, based on the previously developed 2NN MEAM potentials for pure tungsten[10] and carbon[11] by Lee *et al.*, is proposed in this paper.

The rest of this paper is organized as follows. In the next section a brief description of the 2NN MEAM formalism for alloy systems and the procedure for the determination of potential parameters will be given. In Sec. III the fundamental physical properties of the W-C system, especially the interaction between carbon atoms and various defects, are presented and compared with available experimental or other calculation results. Section IV concludes the present work.

II. INTERATOMIC POTENTIAL

A. MEAM potential formalism

MEAM has been reviewed many times before, and more details are available in the literature.[10–12] Here, only the reference structure and the form of the Rose energy function used in this work is described. In the MEAM formalism, pair interaction between different elements could be determined by the energy difference between the total energy per atom of the reference structure estimated from the zero-temperature universal equation of state of Rose *et al.*[13] and the embedding energy. In this paper, a hypothetical $B1$-type WC ordered

TABLE I. MEAM potential parameters for pure W and C. The unit of cohesive energy E_c and the lattice constant of reference structure are eV and Å respectively.

	E_c	r_e	α	δ	A	$\beta^{(0)}$	$\beta^{(1)}$	$\beta^{(2)}$	$\beta^{(3)}$	$t^{(1)}$	$t^{(2)}$	$t^{(3)}$	$C_{\min}$
W	8.66	3.1638	5.6807	0.0	0.40	6.54	1.0	1.0	1.0	−0.60	−0.30	−8.70	0.49
C	7.37	3.5564	4.3652	0.0	1.18	4.25	2.8	2.0	5.0	3.20	1.44	−4.48	1.41

structure is used as the reference structure. The universal equation of state for the $B1$-type WC is given by[11]

$$E^u(R) = -E_c(1 + a^* + \delta a^{*3})e^{-a^*}$$

with

$$a^* = \alpha(R/r_e - 1)$$

and

$$\alpha = \left(\frac{9B\Omega}{E_c}\right)^{1/2},$$

where E_c is the cohesive energy in the reference structure, δ is an adjustable parameter, r_e is the equilibrium nearest-neighbor distance, B is the bulk modulus, and Ω is the equilibrium atomic volume of the reference structure. The parameters of the universal equation of state of hypothetical $B1$-WC are assumed or determined by experiments or high-level calculations, and then the pair interaction between W and C is determined as a function of interatomic distance R.

B. Potential parameters for the W-C system

The potential parameters for tungsten and carbon were taken from Lee *et al.*[10,11] without any modification. The 2NN MEAM potential parameters for pure tungsten and carbon are listed in Table I.

Thirteen model parameters, E_c, r_e, α, δ, $C_{\min}$, $C_{\max}$, and ρ_0 (there are four binary $C_{\min}$ and $C_{\max}$ respectively), must be determined in order to describe the W-C binary system. The first three are material properties, and can be related to the cohesive energy, lattice constant, and bulk modulus of the reference structure. The eight angular-dependent terms ($C_{\min}$ and $C_{\max}$) control the extent of screening of an atom due to its neighboring atoms. Eight other properties were selected to fit those angular-dependent parameters: the formation energy a single C atom in an octahedral site, migration energy of an interstitial C atom in bcc W, binding energy of a single C atom with a vacancy both in the substitutional and deviate site, and lattice constant, cohesive energy, bulk modulus, melting point of B_h WC crystalline. The δ parameter is usually determined according to the $\partial B/\partial P$ value of the reference structure. As the reference structure used here is not a realistic phase, an average value of pure elements was given to δ. The last parameter ρ_0 was changed slightly for a better overall agreement.

In general, there is no simple analytic formula between each parameter and target property, but the effects of some parameters are only confined to a few properties. Table II shows the relationship between parameters and target properties. Here, the $\surd$ sign means the effect is significant, the $-$ sign means the effect is minor, and the $\times$ sign means there is no effect. According to the relationships in Table II, an iterative numerical procedure was used to determine the parameters by fitting to the above-mentioned experimental or first-principles calculated physical properties of W-C systems. The final parameters for the W-C system are shown in Table III.

III. RESULTS AND DISCUSSION

In this section, the potentials are used to calculate the properties of the W-C system and compared with experimental results or other calculations. All the calculations were carried out using the LAMMPS code[14] with the initial temperature of 0 K under periodic boundary conditions. A $20 \times 20 \times 20$ supercell was used for C_nV_m binding-energy calculations, and a $10 \times 10 \times 10$ supercell for others. It has been confirmed that all calculation results are independent of the size of supercell. For computational convenience, a radial cutoff, whose size is between the second and third nearest-neighbor distance, of 4.8 Å was used in order to minimize the effect of third-nearest-neighbor interaction.[10]

A. Carbon in bcc W

In order to evaluate the reliability of the above potentials, we first calculate the interstitial solid solution behaviors of carbon atoms in a bcc W matrix. These properties calculated from the present 2NN MEAM are shown in Table IV, together with data from experiments and first-principles calculations. The corresponding data[15] from the bond order potentials (BOPs)

TABLE II. Effect of parameters on individual properties in W-C systems. The $\surd$ sign means the effect is significant, the $-$ sign means the effect is minor, and $\times$ sign means there is no effect. $E_c^{B_h}$: cohesive energy of hexagonal WC; $r_e^{B_h}$: lattice constant of hexagonal WC; B_{B_h}: bulk moduli of hexagonal WC; $T_m^{B_h}$: melting point of hexagonal WC; E_f^{octa}: formation energy of C in an octahedral site; E_m^C: migration energy of C in bcc W; E_b^{V-C}: carbon-vacancy binding energy.

	$E_c^{B_h}$	$r_e^{B_h}$	B_{B_h}	$T_m^{B_h}$	E_f^{octa}	E_m^C	E_b^{V-C}
E_c	$\surd$	$\surd$	$\surd$	$\surd$	$\surd$	$\surd$	$\surd$
r_e	$\surd$	$\surd$	$\surd$	$\surd$	$\surd$	$\surd$	$\surd$
α	$\surd$	$\surd$	$\surd$	$\surd$	$\surd$	$\surd$	$\surd$
δ	$\surd$	$\surd$	$\surd$	$\surd$	$\surd$	$\surd$	$\surd$
$C_{\min}^{(WWC)}$	$\surd$	$-$	$\surd$	$\surd$	$\surd$	$-$	$\surd$
$C_{\min}^{(CCW)}$	$-$	$-$	$-$	$\surd$	$\surd$	$-$	$\surd$
$C_{\min}^{(WCW)}$	$\times$	$\times$	$\times$	$\surd$	$-$	$-$	$-$
$C_{\min}^{(WCC)}$	$\times$	$\times$	$\times$	$\surd$	$\times$	$\times$	$\times$
$C_{\max}^{(WWC)}$	$-$	$-$	$-$	$\surd$	$\surd$	$-$	$\surd$
$C_{\max}^{(CCW)}$	$-$	$-$	$-$	$\surd$	$\surd$	$\surd$	$\surd$
$C_{\max}^{(WCW)}$	$\times$	$\times$	$\times$	$\surd$	$-$	$-$	$-$
$C_{\max}^{(WCC)}$	$\times$	$\times$	$\times$	$\surd$	$\times$	$\times$	$\times$
ρ_0	$-$	$-$	$-$	$\surd$	$\surd$	$\surd$	$\surd$

TABLE III. MEAM potential parameters for the W-C system.

E_c	r_e	α	δ	$C_{\min}^{(WWC)}$	$C_{\min}^{(CCW)}$	$C_{\min}^{(WCW)}$	$C_{\min}^{(WCC)}$	$C_{\max}^{(WWC)}$	$C_{\max}^{(CCW)}$	$C_{\max}^{(WCW)}$	$C_{\max}^{(WCC)}$	ρ_0
7.977	2.174	6.165	0.00	0.755	0.951	0.052	0.413	1.374	3.644	1.638	3.018	10.461

are also presented for comparison. The first four quantities are fitted target values, and the others are prediction.

The formation energy of a carbon atom in the intrinsic W is defined as

$$E_f^C = E(NW,C) - N\mu_W - \mu_C,$$

where $E(NW,C)$ is the total energy of the supercell containing N W atoms and one C atom, μ_W and μ_C are the chemical potential of W and C, respectively. As can be seen from Table IV, an interstitial carbon atom is energetically more favorable sitting at the octahedral interstitial site with a solution energy of 0.995 eV in reference to the C chemical potential $\mu_C = -7.37$ eV,[20] which is in good agreement with the thermodynamic assessment (0.997 $\pm$0.131 eV) results[16] and first-principles calculation results [0.78 eV (Ref. 5) and 0.82 eV (Ref. 7)].

The binding energy $E_b^{C\text{-}C}$ between two C atoms in bcc W is defined as

$$E_b^{C\text{-}C} = 2E_{NW,C}^{\text{octa}} - E(NW,2C) - N\mu_W,$$

where $E_{NW,C}^{\text{octa}}$ and $E(NW,2C)$ are the energy of the supercell with one octahedral interstitial C atom and two C atoms, respectively. Here, a positive binding-energy indicates attraction between C atoms, while negative indicates repulsion. The most stable configuration for double carbon atoms in bcc W is paired up at two second-nearest-neighboring octahedral sites along the $\langle 100 \rangle$ direction. The predicted binding energy of the C-C cluster is 0.58 eV, which is comparable with the first-principles calculation results [0.5 eV (Ref. 5) and 0.49 eV (Ref. 7)]. A positive binding energy between carbon atoms in C-C cluster indicates that there is an attractive interaction between C atoms in bcc W and might lead to the precipitation of carbides in metallic tungsten. The distance between carbon atoms is 2.689 Å, which is close to the distance between a carbon atom and the nearest carbon atoms (2.795 Å) in hexagonal WC, while it is 3.043 Å in α W_2C. Besides, the distance between a carbon atom in C-C clusters and the third nearest W atom is 2.191 Å, which is also very close to the distance between a carbon atom and the nearest tungsten in hexagonal WC (2.197 Å). This result explains the recent experimental observation[4] that hexagonal WC (not W_2C) formed in bcc W with 0.1–0.8% carbon.

The migration energy of a carbon atom in bcc W is defined as the energy difference between an interstitial carbon atom in an octahedral site and a tetrahedral site. An MD simulation at 2000 K of a 16 000-atom bcc W lattice containing a single carbon interstitial also showed that a C atom migrates exclusively from an octahedral to adjacent octahedral site via a tetrahedral intermediary with our potentials. Experimental data for the migration energy show a large scattering, ranging from 1.64 to 2.15 eV.[9,17,18] This wide experimental range is attributed to difficulties in preparing high-purity bcc W. First-principles calculations both give similar low values, 1.46 eV (Ref. 5) and 1.47 eV.[7] Here, the lowest experimental value [1.64 eV (Ref. 9)] was taken as the target value. The present potentials well reproduces this migration energy (1.69 eV). Such a large energy barrier shows that it is difficult for an interstitial C atom to migrate at lower temperature.

For the carbon-vacancy interaction, similar to the Fe-C system,[21] the carbon atom is not located on the center of the vacancy, but deviates from the vacancy center to bond with the neighboring W in the vicinity of the vacancy and forms an asymmetric C_1V_1 pair in the $\langle 001 \rangle$ direction, as shown in Fig. 1. The distance from a carbon atom in the center of a vacancy to the first-nearest-neighbor (1NN) and 2NN tungsten atoms is 2.585 and 3.213 Å, and 1.972 and 2.135 Å for the carbon atom in the deviate site, respectively. The ground-state structure of WC has a hexagonal symmetry, and the distance between a carbon atom and the nearest tungsten is 2.197 Å, which is very close to the distance between a carbon atom

TABLE IV. Physical properties of carbon atoms in bcc tungsten. E_f^{octa}: formation energy of C in an octahedral site; E_f^{tetra}: formation energy of C in a tetrahedral site; E_m^C: migration energy of C in bcc W; $E_b^{V\text{-}C(\text{sub})}$: carbon-vacancy binding energy in a substitutional site; $E_b^{V\text{-}C(\text{der})}$: carbon-vacancy binding energy in a deviate site; $d_{V\text{-}C}^{\text{der}}$: carbon-vacancy binding distance in a deviate site; $E_b^{C\text{-}C}$: binding energy of most stable double C atoms in bcc W; $E_b^{C\text{-}SIA}$: binding energy of C-SIA cluster in bcc W. The properties marked with a "*" are those used in the fitting process.

	Expt.	MEAM	DFT	BOP (Ref. 15)
$E_f^{\text{octa}*}$ (eV)	0.997 $\pm$ 0.131 (Ref. 16)	0.995	0.78 (Ref. 5) 0.82 (Ref. 7)	2.57
E_m^{C*} (eV)	1.64 (Ref. 9) 1.75 (Ref. 17) 2.15 (Ref. 18)	1.69	1.46 (Ref. 5) 1.47 (Ref. 7)	0.34
$E_b^{V\text{-}C(\text{sub})*}$ (eV)		0.038	0.040 (Ref. 5)	
$E_b^{V\text{-}C(\text{der})*}$ (eV)		2.36	2.33 (Ref. 5) 2.37 (Ref. 7)	1.21
E_f^{tetra} (eV)		2.68	2.24 (Ref. 5) 2.29 (Ref. 7)	2.91
$d_{V\text{-}C}^{\text{der}}$ (Å)		1.26	1.31 (Ref. 5)	1.05
$E_b^{C\text{-}C}$ (eV)		0.58	0.50 (Ref. 5) 0.49 (Ref. 7)	
$E_b^{C\text{-}SIA}$ (eV)		1.13	1.15 (Ref. 19)	

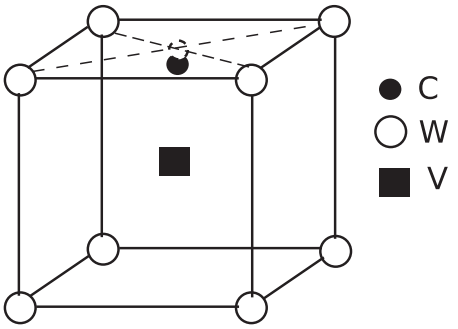

FIG. 1. The most stable structure (deviate site) of a C-V cluster according to the present potential.

in the deviate site and its 2NN tungsten atoms. Therefore, carbon atoms energetically prefer to deviate from the center of vacancy to bond with their neighboring tungsten atoms, further decreasing total energy. As can be seen in Table IV, not only the formation energy of a substitutional C atom in the deviate site but also the distance between a carbon and vacancy is in excellent agreement with the first-principles calculations. It should be noted that the value of substitutional C formation energy from the first-principles calculations in Table IV is 0.4 eV higher than the original values reported in Refs. 5 and 7. This is because the vacancy formation energy obtained with the first-principles calculations is 3.11 eV (Ref. 5) and 3.2 eV,[7] which is about 0.8 eV lower than the experimental value [3.95 eV (Ref. 22)]. In order to describe both the binding energy of a C atom to a vacancy and its substitutional energy simultaneously, the first-principles calculation results were increased by half of the vacancy formation energy difference between the experimental value and first-principles calculation results. For a similar reason, the binding energy of a C-SIA cluster in bcc W in Table IV is 0.53 eV higher than the native value reported in Ref. 19.

The above results show that carbon atoms can be trapped by a vacancy in bcc W. Such bonding between carbon and vacancy will lead to the formation of C_nV_m complexes and influence the physical properties of materials. The new W-C 2NN MEAM potential was then used to study the properties of C_nV_m clusters. The dependence of binding energy of additional C atoms and vacancies to a C_nV_m were investigated as a function of cluster size. First, starting from a single vacancy, the W atom with the highest potential energy was removed. The size of void V_m is gradually increased until m equal 5 by repeating this scheme. For each void size, C atoms were introduced randomly in the vicinity of a vacancy site up to a C-to-V ratio equal to 10. Then, the system was relaxed at 1000–2500 K for 10 ps, and quenched to 0 K. The orientation of the stable cluster was rotated 30° and 60° respectively, and then processed by quenched annealing in order to ensure the cluster obtained in this way is stable.

The binding energy of a carbon atom or a vacancy to a C_nV_m cluster was derived according to the following definition:

$$E^{C}_{b,C_nV_m} = E(C_{n-1}V_m) + E^{\mathrm{oct}}_{C} - E(C_nV_m),$$

$$E^{V}_{b,C_nV_m} = E(C_nV_{m-1}) + E^{V}_{f} - E(C_nV_m),$$

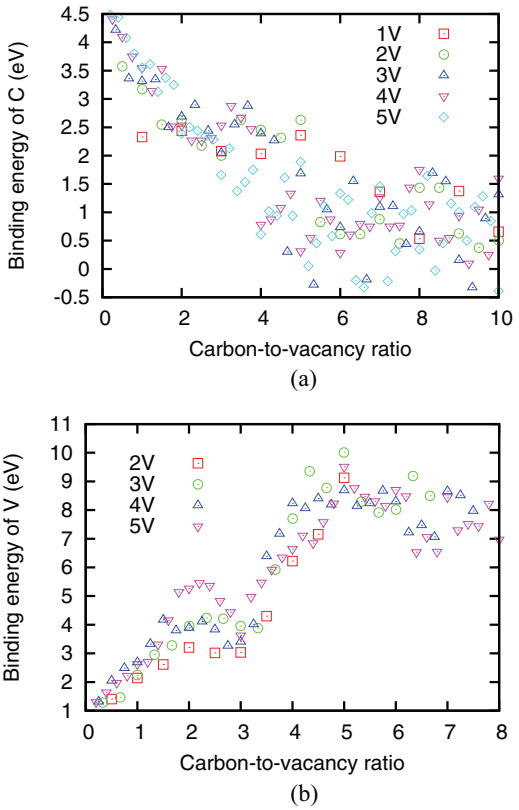

FIG. 2. (Color online) Binding energies in eV of a carbon atom or vacancy from a C_nV_m cluster as a function of the carbon-to-vacancy ratio n/m. (a) Binding energies of carbon. (b) Binding energies of vacancy.

where E^{C}_{b,C_nV_m} is the binding energy of a carbon atom to a C_nV_m cluster, E^{V}_{b,C_nV_m} the binding energy of a vacancy to a C_nV_m cluster, $E(C_nV_m)$ the total energy of the supercell with a C_nV_m cluster optimized according to the procedure described above, E^{oct}_{C} the formation energy of a C atom in an octahedral site and E^{V}_{f} the formation energy of a vacancy in bcc W. The results for the binding energy of C atoms or vacancies in C_nV_m clusters are presented in Fig. 2.

From Fig. 2, it can be seen that the binding energies mainly depend on the ratio between carbon atoms and vacancies in a C_nV_m cluster. The binding energy of carbon atoms in a carbon-vacancy cluster decreases with the carbon density, because the additional C atoms decrease the free space of C_nV_m clusters and the repulsive interaction between carbon atoms will be significant. It shows that the C atom is most strongly bound to the large nearly empty voids. On the contrary, the binding energy of a vacancy gradually increases with increasing the carbon density, followed by a slightly decrease at carbon density greater than 5. The change in the binding energy of vacancies may be originated from the self-trapping mechanism,[23] which decreases the carbon density. That is, the carbon atoms produce pressure large enough to push lattice atoms off their normal sites and result in a "near-Frenkel-pair" defect in the near vicinity of the cluster, therefore increasing the bubble volume and thus lowering the carbon density. For a carbon-to-vacancy ratio of 5, the binding energy of C atoms remains largely positive, which

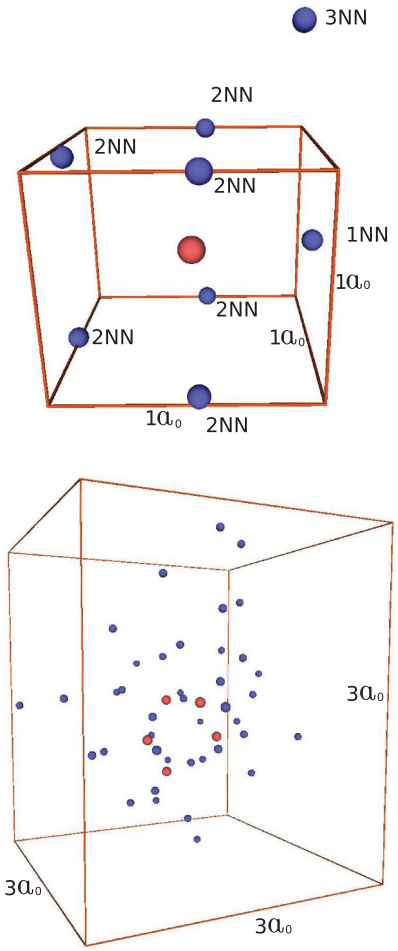

FIG. 3. (Color online) The stable configurations of C_8V_1 and $C_{40}V_5$. The larger ones represent vacancies, smaller carbon atoms. a_0 is the lattice constant of bcc W. (a) C_8V_1; (b) $C_{40}V_5$.

indicates the strong tendency of carbon to aggregate in bcc W. Such a microstructural complexity governs the performance of materials.[24] The maximum binding energy of a carbon atom or a vacancy in a carbon-vacancy cluster is about 4.5 and 10 eV, respectively. The maximum binding energy for carbon is determined by the the energy difference between a carbon atom in an octahedral site and the most stable structure of a carbon atom on the surface of bcc W, which is about 4.78 eV.[25] The maximum binding energy of a vacancy cannot be related to other physical properties directly. Figure 3 shows the stable geometries for a W vacancy surrounded by up to eight C atoms. In the C_8V_1 cluster, carbon atoms first occupy the nearest (1NN) octahedral interstitial sites, followed by the second-nearest (2NN) octahedral sites. When the number of carbon atoms surpass 7, because of the strong repulsion between carbon atoms, one of them jumps to a third-nearest (3NN) octahedral site. The stable $C_{40}V_5$ cluster consists of five vacancies at the nearest-neighbor lattice sites, and the carbon atoms locate in the vicinity of octahedral interstitial sites around the vacancies.

The interaction between self-interstitial atoms (SIAs) and carbon atoms is also important in irradiated samples. Besides, they represent a simple model for binding carbon to overcoordinated defects such as grain boundaries and dislocations. Previous studies[7,26] have revealed that the most stable shape of a self-interstitial in bcc is a ⟨111⟩ crowdion. Here, one ⟨111⟩ SIA is introduced, and then one C atom is placed in the vicinity of the SIA. After full relaxation, the binding energy of one C atom and one SIA is calculated according to the following definition:

$$E_b^{C\text{-}SIA} = E(C_1) + E(SIA_1) - E(C_1SIA_1) - \mu_W \delta n_W,$$

where $E(C_1SIA_1)$, $E(C_1)$, $E(SIA_1)$ denote the total energy of the supercell with one C_1-SIA_1, C atom, and SIA, respectively, μ_W is the chemical potential of W, and δn_W is the difference in atom number of W. The first-principles calculations[19] show a strong binding between a self-interstitial and an interstitial carbon atom. The present potential also successfully predicts a strong binding between a SIA and a nearby C atom with a binding energy of 1.13 eV, which is in good agreement with the first-principles calculation results (1.15 eV).[19] A positive binding energy indicates that there is an attractive interaction between SIAs and C atoms, which will increase the migration energy barrier of SIA. This is consistent with experiments[27] and calculation results[19] which show that a small amount of carbon impurities can significantly increase the release temperature of SIAs by about 200 K in bcc W. The distances between the carbon atom and SIA in C-SIA clusters is 2.202 Å, which is very close to the distance between a carbon atom and the nearest tungsten in hexagonal WC (2.197 Å). The positive binding energy of a C-SIA cluster and the hexagonal WC-like local structure may account for the initial formation of hexagonal WC in bcc W.

The effects of vacancy-carbon clusters on the diffusivity in bcc W, which is a critical factor in controlling microstructure evolution and changing mechanical properties, were studied via the nudged elastic band (NEB) method[28,29] by calculating the activation barriers of migration. In the NEB calculations, a set of intermediate states are distributed along the reaction coordinate from known initial state to final state. To ensure the continuity, images are coupled with elastic forces and each intermediate state is fully relaxed in the hyperspace perpendicular to the reaction path. Isolated point defects, C_1 and V_1, are the simplest point defects in bcc W, and thus the migration mechanisms are simpler compared to the large C_nV_m clusters. As discussed above, the energy difference between the octahedral and the tetrahedral site should be a good estimate of the migration energy for the single (octahedral) C interstitials. We indeed find the tetrahedral carbon site as the saddle point in the NEB calculation for C migration from one octahedral site to the nearest octahedral site in vacancy-free bcc W along the ⟨100⟩ direction. The calculated migration energy is 1.69 eV (as shown in Fig. 4), which agrees well with the experimental value [1.64 eV (Ref. 9)]. Regarding the migration of vacancy, there are two possible migration paths for a single vacancy in bcc W: along the ⟨100⟩ and ⟨111⟩ directions. The migration pathways for a single vacancy along the ⟨100⟩ and ⟨111⟩ directions are shown in Fig. 4. In comparison, diffusion along the ⟨111⟩ direction requires smaller energy, and is thus the minimum-energy pathway for vacancy diffusion. The calculated migration barrier along the ⟨111⟩ direction is 1.87 eV, which is in good agreement with experimental data ranging from 1.8 to 2.02 eV.[30,31]

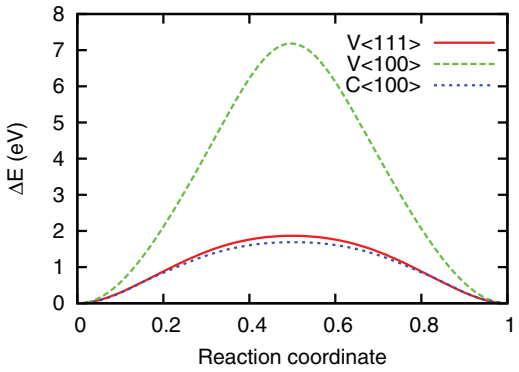

FIG. 4. (Color online) Migration of isolated point defects, C_1 and V_1.

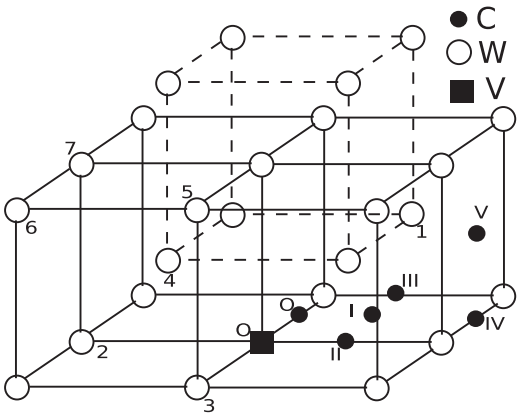

FIG. 5. Positions of carbon and vacancy for possible dissociative and associative migration of C_1V_1 cluster. Position O represents the origin. Point defects are indicated by Roman (carbon) and Arabic (W vacancy) numerals.

The number of possible migration pathways increases rapidly with defect cluster size. Figure 5 shows the positions of a carbon and vacancy for possible dissociative and associative migration of a C_1V_1 cluster. The energy paths are shown in Figs. 6 and 7 and the migration barriers are tabulated in Table V. The energetically favorable dissociation pathway for carbon atom in C_1V_1 clusters is $O \rightarrow$ I $\rightarrow$ IV (as shown in Fig. 5) with an activation energy of 3.99 eV (as shown in Fig. 8). The migration barriers for a vacancy to jump to nearest neighbors in C_1V_1 clusters show a large scattering, ranging from 2.47 to 8.18 eV. The minimum-energy path is $O \rightarrow 4 \rightarrow 7$. The activation energy is 4.16 eV, which is about 0.17 eV larger than that of the C atom, and thus for carbon atoms it is easier to jump away from the C_1V_1 cluster than the vacancy. The minimum-energy dissociative profile for a C atom or vacancy in the C_1V_1 cluster is shown in Fig. 8.

One interesting result is that for all dissociative carbon atom migration pathways, the migration barrier for a carbon atom to jump away from a vacancy is much larger than the carbon atom jump toward a vacancy, which means that a carbon atom energetically prefers to rebind to the vacancy than to dissociate from the vacancy. In contrast to the dissociative migrations, the associative C_1V_1 cluster migration requires much higher energy (as shown in Fig. 7). By comparison of the migration barriers of C_1V_1 clusters to that of isolated point defects, it was found that the migration barriers of vacancy-carbon clusters are significantly higher compared to that of a monovacancy. This leads to decreased self-diffusivity in bcc W with increasing carbon content.

B. Tungsten carbides

It has been shown that the present 2NN MEAM potential provides a very good description of the properties of carbon as an interstitial solute element in bcc W, and can be used reliably to investigate the interaction between carbon atoms and other defects such as vacancies, dislocations, and grain boundaries. As a means of checking the transferability of the present potential, the formation energies, lattice parameters, and bulk modulus of several tungsten carbides (WC and W_2C) were calculated. The ground state of tungsten carbide (B_h WC) is a hexagonal structure with space-group symmetry $P\bar{6}m2$. Only the cohesive energy, lattice parameters, and bulk modulus of B_h WC were used during the fitting process. Although the equilibrium volume, cohesive energy, and bulk modulus of the $B1$-type WC are directly related to MEAM parameters, those properties were not used during the fitting process, for $B1$ WC is a high-temperature phase and its properties are hard to obtain experimentally. The B_h WC, α W_2C, and β W_2C are real carbides, and the calculation results could be compared with experiments. The $B2$ and $B3$ WC do not exist in the real phase diagram, but the cohesive energy, lattice parameters, and bulk modulus were reported in references by first-principles and bond order potentials (BOP) calculations.

In Table VI the lattice parameters, cohesive energies, and elastic constants of several existing and hypothetical tungsten carbides calculated using the 2NN MEAM potentials (shown in Tables I and III) are presented with data from experiments or other calculations, which show good agreement between

TABLE V. Migration energy barriers for C_1V_1 cluster. E_m: migration energy.

Carbon atom jump	E_m (eV)	Vacancy jump	E_m (eV)	Associative migration	E_m (eV)
$O \rightarrow$ I	0.437	$O \rightarrow 1$	3.960	$C_1(O)V_1(O) \rightarrow C_1(\mathrm{I})V_1(1)$	5.251
$O \rightarrow$ II	0.509	$O \rightarrow 2$	8.182	$C_1(O)V_1(O) \rightarrow C_1(\mathrm{I})V_1(3)$	4.959
$O \rightarrow$ III	3.094	$O \rightarrow 3$	7.753		
I $\rightarrow$ III	3.029	$O \rightarrow 4$	2.473		
I $\rightarrow$ IV	2.808	$4 \rightarrow 5$	1.843		
IV $\rightarrow$ V	1.69	$4 \rightarrow 6$	1.897		
		$4 \rightarrow 7$	1.804		

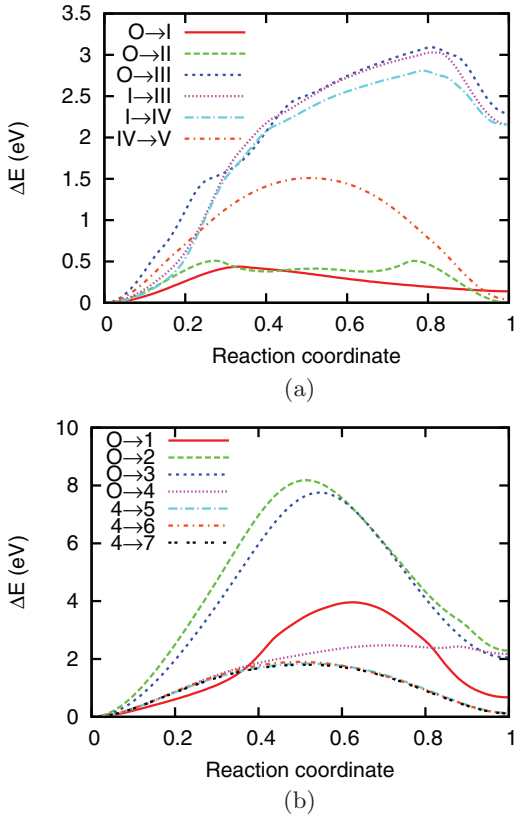

FIG. 6. (Color online) Barriers for migrations of the C_1V_1 clusters. (a) Migration barriers of C atoms. (b) Migration barriers of vacancies.

the reference data and the MEAM calculations. The formation energies were used to evaluate the relative stabilities of WC polymorphs. These energies were estimated using the formal reaction:

$$W + C(\text{graphite}) \rightarrow B_h \quad WC, B1 \quad WC.$$

The results are as follows: $E_{\text{form}}(B_h \quad WC) = -0.56$ eV and $E_{\text{form}}(B1 \quad WC) = 0.1$ eV per formula unit, which shows that the B_h WC is a stable phase and a metastable character of the $B1$ WC. As for $B2$ and $B3$ WC, all of them are not stable carbides in the W-C system. The agreement between 2NN MEAM and DFT is quite satisfactory. The 2NN MEAM results preserve the order of stability predicted by the DFT

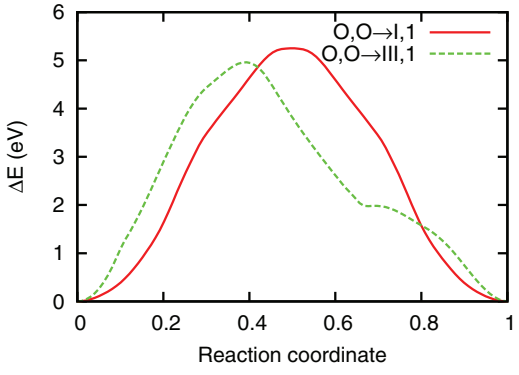

FIG. 7. (Color online) Associative migrations of the C_1V_1 clusters.

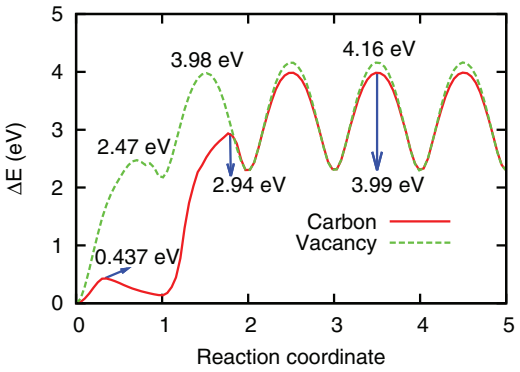

FIG. 8. (Color online) The minimum-energy dissociation profile of a carbon atom or vacancy in C_1V_1 clusters.

calculations. The difference in the cohesive energy per formula unit from the 2NN MEAM and DFT results are less than 0.3 eV at most. The lattice parameters predicted by the 2NN MEAM also agree with the DFT results. The melting temperature of B_h WC, which is especially important to radiation damage simulations with energies above 1 keV, was evaluated to be 2800 ± 50 K with the present potential by two-phase simulations,[38] which agrees well with the experimental value of 3000–3050 K.[39]

Next we discuss the M_2C-type tungsten carbide. The formation energies of α W_2C are about -0.3161 ± 0.0041 eV,[16] or 0.063–0.065 eV,[32,36] for the reference states of bcc W and graphite carbon at 0 K accessed by thermodynamics and first-principle calculations, respectively. The present 2NN MEAM potentials predicts a value of -0.3466 eV at 0 K. Moreover, the formation energy of α W_2C is still above the tie line connecting B_h WC and pure tungsten, which is consistent with the experiments that the low-temperature W_2C structure is actually a mixture of pure tungsten and B_h WC, while α W_2C is a high-temperature phase.[39] This potential also gives comparable lattice parameters and bulk modulus with experimental or first-principles calculation results for α W_2C. As can be seen from Table VI, the formation energy of β W_2C is about -0.0972 eV, which is in good agreement with previous first-principles calculations.[32,36] The bulk modulus by 2NN MEAM is consistent with DFT results.[32] The calculated lattice parameters of β W_2C is within 5% of that seen in experiment.[33] It should be noticed that none of this information was considered during the parameter optimization. Based on the formation energies estimations, the W-C phases may be placed in the following sequence according to their stability: $B_hWC > \alpha W_2C > \beta W_2C > B1WC$, which differs from the result obtained by first-principles calculations ($B_hWC > \beta W_2C > \alpha W_2C > B1WC$).[32,36] Our results are consistent with the experiments which show that βW_2C is not stable and will transform into α W_2C during cooling.[37,39] Experiments[40] also show that β W_2C is unstable and upon mechanical working is converted to α W_2C.

The ability of the 2NN MEAM potentials presented in this work to reproduce physical properties of both the MC- and M_2C-type tungsten carbides shows that it has a satisfactory transferability, and can be used to analyze interaction between W and C over a large composition range.

TABLE VI. Comparison of properties of several existing and hypothetical tungsten carbides obtained from experiments, MEAM (this work), and other calculations. E_c: cohesive energy per formula unit (eV/f.u.); B: bulk modulus (GPa); ΔE: energy difference with respect to ground-state structure (eV/f.u.); ΔH: formation enthalpy (eV/f.u.); c/a: axial ratio of hexagonal tungsten carbide; V: volume (Å^3/f.u.). The properties marked with a "*" are those used in the fitting process.

	Expt.	MEAM	DFT	BOP (Ref. 8)
Rocksalt ($B1$)				
ΔE		0.65	0.95 (Ref. 8) 0.9 (Ref. 32)	0.98
a		4.3707	4.482 (Ref. 8) 4.351 (Ref. 32)	4.380
B		525	346 (Ref. 8) 374 (Ref. 32)	405
Cesium chloride ($B2$)				
ΔE		2.02	2.32 (Ref. 8)	2.32
a		2.733	2.779 (Ref. 8)	2.704
B		491	350 (Ref. 8)	411
Zinc blende ($B3$)				
ΔE		1.69	1.87 (Ref. 8)	2.12
a		4.6948	4.801 (Ref. 8)	4.679
B		303	246 (Ref. 8)	511
Tungsten carbide (B_h)				
E_c*	16.68	16.59	15.01 (Ref. 8) 21.28 (Ref. 32)	16.68
a*	2.907 (Ref. 33)	2.945	2.979 (Ref. 8) 2.906 (Ref. 32)	2.917
c/a*	0.976 (Ref. 33)	0.949	0.975 (Ref. 8) 0.9721 (Ref. 32)	0.964
B*	443 (Ref. 34) 402 (Ref. 35)	459	368 (Ref. 8) 400 (Ref. 32)	443
(αW_2C)				
ΔH	-0.3161 ± 0.0041 (Ref. 16)	-0.3466	0.065 (Ref. 32) 0.063 (Ref. 36)	
a	2.996 (Ref. 33)	2.9245	3.043 (Ref. 32) 2.985 (Ref. 36)	
c/a	1.577 (Ref. 33)	1.7123	1.5307 (Ref. 32) 1.5735 (Ref. 36)	
B	338 (Ref. 35) 336 (Ref. 37)	428	343 (Ref. 32)	
(βW_2C)				
ΔH		-0.0972	-0.018 (Ref. 32) -0.007 (Ref. 36)	
a	4.719 (Ref. 33)	4.9178	4.725 (Ref. 32) 4.728 (Ref. 36)	
b	6.017 (Ref. 33)	5.9207	6.057 (Ref. 32) 6.097 (Ref. 36)	
c	5.181 (Ref. 33)	5.1368	5.195 (Ref. 32) 5.227 (Ref. 36)	
B		406	353 (Ref. 32)	

IV. CONCLUSIONS

An empirical many-body interatomic potential for the W-C system has been developed based on the 2NN MEAM formalism, which can not only be employed to study the behavior of carbon atoms in bcc tungsten, but also the energetics and structural properties of tungsten carbides. This potential provides a good description of various physical properties of the W-C system, such as the formation energy of interstitial carbon atoms, the migration energy of carbon atoms in bcc tungsten and lattice parameters, bulk modulus, cohesive energy of several tungsten carbides. It is expected that the potential developed herein allows us to correctly survey interaction between W and C over a large composition range, many of which are intractable with previous potentials. The stability of carbon-vacancy clusters in bcc tungsten was also studied using this potential. It appears that the dissociation energies mainly depend on the carbon-to-vacancy ratio rather than the cluster size. Beside, a positive attractive interaction in C-C and SIA-C clusters was found in bcc W, and both the C-C cluster and C-SIA cluster form a hexagonal WC-like local structure, which may account for the initial precipitation of carbides in metallic tungsten.

ACKNOWLEDGMENTS

This work was partially financially supported by the Science and Technology Foundation of China Academy of Engineering Physics and the National Natural Science Foundation of China under Contract Nos. 11305147 and 91226203.

*pichen@mappi.helsinki.fi

[1]R. Neu, R. Dux, A. Geier, O. Gruber, A. Kallenbach, K. Krieger, H. Maier, R. Pugno, V. Rohde, and S. Schweizer, Fusion Eng. Des. **65**, 367 (2003).

[2]R. Mitteau, J. Missiaen, P. Brustolin, O. Ozer, A. Durocher, C. Ruset, C. Lungu, X. Courtois, C. Dominicy, H. Maier, C. Grisolia, G. Piazza, and P. Chappuis, Fusion Eng. Des. **82**, 1700 (2007).

[3]C. S. Harte, C. Suzuki, T. Kato, H. Sakaue, D. Kato, K. Sato, N. Tamura, S. Sudo, R. D'Arcy, E. Sokell *et al.*, J. Phys. B **43**, 205004 (2010).

[4]Y. Ueda, M. Fukumoto, I. Sawamura, D. Sakizono, T. Shimada, and M. Nishikawa, Fusion Eng. Des. **81**, 233 (2006).

[5]Y. L. Liu, H. B. Zhou, J. Shuo, Y. Zhang, and G. H. Lu, J. Phys.: Condens. Matter **22**, 445504 (2010).

[6]Y. L. Liu, H. B. Zhou, Y. Zhang, G. H. Lu, and G. N. Luo, Comput. Mater. Sci. **50**, 3213 (2011).
[7]X. S. Kong, Y. W. You, C. Song, Q. F. Fang, J. L. Chen, G. N. Luo, and C. S. Liu, J. Nucl. Mater. **430**, 270 (2012).
[8]N. Juslin, P. Erhart, P. Traskelin, J. Nord, K. O. Henriksson, K. Nordlund, E. Salonen, and K. Albe, J. Appl. Phys. **98**, 123520 (2005).
[9]A. Shepela, J. Less. Common. Met. **26**, 33 (1972).
[10]B. J. Lee, M. I. Baskes, H. Kim, and Y. K. Cho, Phys. Rev. B **64**, 184102 (2001).
[11]B. J. Lee, Acta Mater. **54**, 701 (2006).
[12]M. I. Baskes, Phys. Rev. B **46**, 2727 (1992).
[13]J. H. Rose, J. R. Smith, F. Guinea, and J. Ferrante, Phys. Rev. B **29**, 2963 (1984).
[14]S. Plimpton, J. Comput. Phys. **117**, 1 (1995).
[15]Z. S. Yang, Q. Xu, J. Q. Liao, Q. Li, G. H. Lu, and G. N. Luo, Nucl. Instrum. Methods Phys. Res., Sect. B **267**, 3144 (2009).
[16]D. K. Gupta and L. L. Seigle, Metall. Mater. Trans. A **6**, 1939 (1975).
[17]I. Kovenski, *Diffusion in Body-Central Cubic Metals* (ASM, Metals Park, OH, 1965), Vol. 283.
[18]L. N. Aleksandrov and V. Y. Shchelkonogov, Soviet Power Metall. Met. C **3**, 288 (1964).
[19]C. S. Becquart, C. Domain, U. Sarkar, A. DeBacker, and M. Hou, J. Nucl. Mater. **403**, 75 (2010).
[20]C. Kittel, *Introduction to Solid State Physics* (Wiley, New York, 1996).
[21]P. Hautojärvi, J. Johansson, A. Vehanen, J. Yli-Kauppila, and P. Moser, Phys. Rev. Lett. **44**, 1326 (1980).
[22]C. J. Smithells, *Smithells Metals Reference Book*, edited by E. A. Brandes and G. B. Brook (Butterworth-Heinemann, Oxford, 1992).
[23]W. D. Wilson, C. L. Bisson, and M. I. Baskes, Phys. Rev. B **24**, 5616 (1981).
[24]C. J. Först, J. Slycke, K. J. Van Vliet, and S. Yip, Phys. Rev. Lett. **96**, 175501 (2006).
[25]H. B. Zhou, S. Jin, Y. Zhang, and G. H. Lu, Sci. China Phys. Mech. **54**, 2164 (2011).
[26]D. Nguyen-Manh, A. P. Horsfield, and S. L. Dudarev, Phys. Rev. B **73**, 020101 (2006).
[27] H. Tanimoto, H. Mizubayashi, H. Nishimura, and S. Okuda, J. Phys. IV **6**, C8-285 (1996).
[28]G. Henkelman, B. P. Uberuaga, and H. Jónsson, J. Chem. Phys. **113**, 9901 (2000).
[29]G. Henkelman and H. Jónsson, J. Chem. Phys. **113**, 9978 (2000).
[30]R. W. Balluffi, J. Nucl. Mater. **69**, 240 (1978).
[31]J. N. Mundy, S. T. Ockers, and L. C. Smedskjaer, Philos. Mag. A **56**, 851 (1987).
[32]Y. F. Li, Y. M. Gao, B. Xiao, T. Min, Z. J. Fan, S. Q. Ma, and L. L. Xu, J. Alloy Compd. **502**, 28 (2010).
[33]V. Kublii and T. Y. Velikanova, Power Metall. Met. C **43**, 630 (2004).
[34]M. Lee and R. Gilmore, J. Mater. Sci. **17**, 2657 (1982).
[35]A. Nino, A. Tanaka, S. Sugiyama, and H. Taimatsu, Mater. Trans. **51**, 1621 (2010).
[36]D. V. Suetin, I. R. Shein, A. S. Kurlov, A. I. Gusev, and A. L. Ivanovskĭ, Phys. Solid State **50**, 1420 (2008).
[37]H. Taimatsu, S. Sugiyama, and Y. Kodaira, Mater. Trans. **49**, 1256 (2008).
[38]U. Landman, W. D. Luedtke, R. N. Barnett, C. L. Cleveland, M. W. Ribarsky, E. Arnold, S. Ramesh, H. Baumgart, A. Martinez, and B. Khan, Phys. Rev. Lett. **56**, 155 (1986).
[39]A. S. Kurlov and A. I. Gusev, Inorg. Mater. **42**, 121 (2006).
[40]G. S. Upadhyaya, *Cemented Tungsten Carbides: Production, Properties and Testing* (William Andrew, New York, 1998).